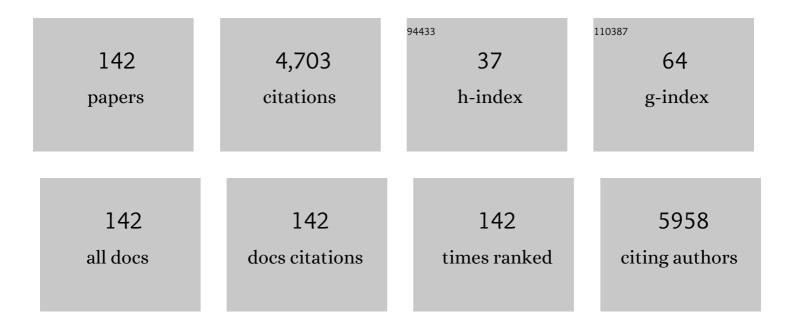
List of Publications by Year in descending order

Source: https://exaly.com/author-pdf/1194611/publications.pdf Version: 2024-02-01



#	Article	IF	CITATIONS
1	Characterization of Nanoscale Mechanical Heterogeneity in a Metallic Glass by Dynamic Force Microscopy. Physical Review Letters, 2011, 106, 125504.	7.8	347
2	Dielectrophoretically Aligned Carbon Nanotubes to Control Electrical and Mechanical Properties of Hydrogels to Fabricate Contractile Muscle Myofibers. Advanced Materials, 2013, 25, 4028-4034.	21.0	236
3	Hybrid hydrogels containing vertically aligned carbon nanotubes with anisotropic electrical conductivity for muscle myofiber fabrication. Scientific Reports, 2014, 4, 4271.	3.3	213
4	Intrinsic correlation between β-relaxation and spatial heterogeneity in a metallic glass. Nature Communications, 2016, 7, 11516.	12.8	197
5	High-Resolution STM and XPS Studies of Thiophene Self-Assembled Monolayers on Au(111). Journal of Physical Chemistry B, 2002, 106, 7139-7141.	2.6	160
6	Hybrid hydrogel-aligned carbon nanotube scaffolds to enhance cardiac differentiation of embryoid bodies. Acta Biomaterialia, 2016, 31, 134-143.	8.3	145
7	Ordered networks of rat hippocampal neurons attached to silicon oxide surfaces. Journal of Neuroscience Methods, 2000, 104, 65-75.	2.5	136
8	Interaction of Ga Adsorbates with Dangling Bonds on the Hydrogen Terminated Si(100) Surface. Japanese Journal of Applied Physics, 1996, 35, L1085-L1088.	1.5	130
9	Microfluidic Spinning of Cellâ€Responsive Grooved Microfibers. Advanced Functional Materials, 2015, 25, 2250-2259.	14.9	130
10	Facile and green production of aqueous graphene dispersions for biomedical applications. Nanoscale, 2015, 7, 6436-6443.	5.6	114
11	Myotube formation on gelatin nanofibers – Multi-walled carbon nanotubes hybrid scaffolds. Biomaterials, 2014, 35, 6268-6277.	11.4	109
12	Multiscale Energy Dissipation Mechanism in Tough and Self-Healing Hydrogels. Physical Review Letters, 2018, 121, 185501.	7.8	104
13	Nanoscopic Investigation of the Self-Assembly Processes of Dialkyl Disulfides and Dialkyl Sulfides on Au(111). Journal of Physical Chemistry B, 2000, 104, 7411-7416.	2.6	85
14	Engineered Nanomembranes for Directing Cellular Organization Toward Flexible Biodevices. Nano Letters, 2013, 13, 3185-3192.	9.1	85
15	Nano-palpation AFM and its quantitative mechanical property mapping. Microscopy (Oxford, England), 2014, 63, 193-208.	1.5	67
16	Gelatin–Polyaniline Composite Nanofibers Enhanced Excitation–Contraction Coupling System Maturation in Myotubes. ACS Applied Materials & Interfaces, 2017, 9, 42444-42458.	8.0	62
17	Nanorheological Mapping of Rubbers by Atomic Force Microscopy. Macromolecules, 2013, 46, 1916-1922.	4.8	61
18	Macrodipole Interaction of Helical Peptides in a Self-Assembled Monolayer on Gold Substrate. Langmuir, 1998, 14, 6167-6172.	3.5	58

#	Article	IF	CITATIONS
19	Visualization of nanomechanical mapping on polymer nanocomposites by AFM force measurement. Polymer, 2010, 51, 2455-2459.	3.8	58
20	Nanorheology of Polymer Blends Investigated by Atomic Force Microscopy. Japanese Journal of Applied Physics, 1997, 36, 3850-3854.	1.5	57
21	Electrically regulated differentiation of skeletal muscle cells on ultrathin graphene-based films. RSC Advances, 2014, 4, 9534.	3.6	57
22	Nanorheological Analysis of Polymer Surfaces by Atomic Force Microscopy. Japanese Journal of Applied Physics, 2005, 44, 5425-5429.	1.5	54
23	Mechanical Regulation of Cellular Adhesion onto Honeycomb-Patterned Porous Scaffolds by Altering the Elasticity of Material Surfaces. Biomacromolecules, 2013, 14, 1208-1213.	5.4	53
24	Dynamic Measurement of Single Protein's Mechanical Properties. Biochemical and Biophysical Research Communications, 2000, 272, 55-63.	2.1	52
25	Observation of gellan gum by scanning tunneling microscopy. Carbohydrate Polymers, 1996, 30, 77-81.	10.2	51
26	Quantitative Nanomechanical Investigation on Deformation of Poly(lactic acid). Macromolecules, 2012, 45, 8770-8779.	4.8	51
27	Production of a cellular structure in carbon nanotube/natural rubber composites revealed by nanomechanical mapping. Carbon, 2010, 48, 3708-3714.	10.3	50
28	True Surface Topography and Nanomechanical Mapping Measurements on Block Copolymers with Atomic Force Microscopy. Macromolecules, 2010, 43, 3169-3172.	4.8	47
29	New Insights into Morphology of High Performance BHJ Photovoltaics Revealed by High Resolution AFM. Nano Letters, 2014, 14, 5727-5732.	9.1	45
30	Characterization of Surface Viscoelasticity and Energy Dissipation in a Polymer Film by Atomic Force Microscopy. Macromolecules, 2011, 44, 8693-8697.	4.8	44
31	Atomic Force Microscopy Nanomechanics Visualizes Molecular Diffusion and Microstructure at an Interface. ACS Macro Letters, 2013, 2, 757-760.	4.8	44
32	Investigation of True Surface Morphology and Nanomechanical Properties of Poly(styrene- <i>b</i> -ethylene- <i>co</i> -butylene- <i>b</i> -styrene) Using Nanomechanical Mapping: Effects of Composition. Macromolecules, 2010, 43, 9049-9055.	4.8	42
33	Single polymer chain rubber elasticity investigated by atomic force microscopy. Polymer, 2006, 47, 2505-2510.	3.8	41
34	Anisotropic thermal expansion in polypropylene/poly(ethylene-co-octene) binary blends: influence of arrays of elastomer domains. Polymer, 2005, 46, 4899-4908.	3.8	39
35	Investigation of Reactive Polymerâ^'Polymer Interface Using Nanomechanical Mapping. Macromolecules, 2010, 43, 5521-5523.	4.8	39
36	Spatial coordination of cell orientation directed by nanoribbon sheets. Biomaterials, 2015, 53, 86-94.	11.4	39

#	Article	IF	CITATIONS
37	Graphene induces spontaneous cardiac differentiation in embryoid bodies. Nanoscale, 2016, 8, 7075-7084.	5.6	39
38	Visualization and Quantification of the Chemical and Physical Properties at a Diffusion-Induced Interface Using AFM Nanomechanical Mapping. Macromolecules, 2014, 47, 3761-3765.	4.8	38
39	Two-dimensional electron gas at the Ti-diffused BiFeO3/SrTiO3 interface. Applied Physics Letters, 2015, 107, .	3.3	38
40	Viscoelasticity of Inhomogeneous Polymers Characterized by Loss Tangent Measurements Using Atomic Force Microscopy. Macromolecules, 2014, 47, 7971-7977.	4.8	37
41	Direct Mapping of Nanoscale Viscoelastic Dynamics at Nanofiller/Polymer Interfaces. Macromolecules, 2018, 51, 6085-6091.	4.8	37
42	Atomic Force Microscopy of Mechanical Property of Natural Rubber. Japanese Journal of Applied Physics, 2005, 44, 5393-5396.	1.5	35
43	Nanorheology measurement on a single polymer chain. Applied Physics Letters, 2002, 81, 724-726.	3.3	34
44	Elastic modulus of ultrathin polymer films characterized by atomic force microscopy: The role of probe radius. Polymer, 2016, 87, 114-122.	3.8	34
45	Characterization of morphology and mechanical properties of block copolymers using atomic force microscopy: Effects of processing conditions. Polymer, 2012, 53, 1960-1965.	3.8	31
46	Exceptionally high nanoscale wear resistance of a Cu47Zr45Al8 metallic glass with native and artificially grown oxide. Intermetallics, 2018, 93, 312-317.	3.9	31
47	Elastic and viscoelastic characterization of inhomogeneous polymers by bimodal atomic force microscopy. Japanese Journal of Applied Physics, 2016, 55, 08NB06.	1.5	30
48	Carbon nanotubes embedded in embryoid bodies direct cardiac differentiation. Biomedical Microdevices, 2017, 19, 57.	2.8	30
49	Dynamic Moduli Mapping of Silica-Filled Styrene–Butadiene Rubber Vulcanizate by Nanorheological Atomic Force Microscopy. Macromolecules, 2019, 52, 311-319.	4.8	29
50	Rectified photocurrent in a protein based molecular photo-diode consisting of a cytochrome b562-green fluorescent protein chimera self-assembled monolayer. Biosensors and Bioelectronics, 2004, 19, 1169-1174.	10.1	28
51	NANOMECHANICS OF THE RUBBER–FILLER INTERFACE. Rubber Chemistry and Technology, 2017, 90, 272-284.	1.2	28
52	Microfluidic Generation of Polydopamine Gradients on Hydrophobic Surfaces. Langmuir, 2014, 30, 832-838.	3.5	27
53	Hydrogels containing metallic glass sub-micron wires for regulating skeletal muscle cell behaviour. Biomaterials Science, 2015, 3, 1449-1458.	5.4	27
54	Liquid Marbles in Nature: Craft of Aphids for Survival. Langmuir, 2019, 35, 6169-6178.	3.5	27

#	Article	IF	CITATIONS
55	Miscibility in blends of poly(3-hydroxybutyrate) and poly(vinylidene chloride-co-acrylonitrile). Journal of Polymer Science, Part B: Polymer Physics, 1997, 35, 2645-2652.	2.1	26
56	Analytical methods to derive the elastic modulus of soft and adhesive materials from atomic force microcopy force measurements. Journal of Polymer Science, Part B: Polymer Physics, 2019, 57, 1279-1286.	2.1	25
57	Dynamic Force Spectroscopy on a Single Polymer Chain. Macromolecules, 2006, 39, 5921-5925.	4.8	24
58	Observation of dynamical heterogeneities and their time evolution on the surface of an amorphous polymer. Soft Matter, 2015, 11, 1425-1433.	2.7	24
59	Fabrication of poly(ethylene glycol) hydrogels containing vertically and horizontally aligned graphene using dielectrophoresis: An experimental and modeling study. Carbon, 2017, 123, 460-470.	10.3	24
60	Nanomechanical Imaging of the Diffusion of Fullerene into Conjugated Polymer. ACS Nano, 2017, 11, 8660-8667.	14.6	24
61	Length scale of mechanical heterogeneity in a glassy polymer determined by atomic force microscopy. Applied Physics Letters, 2012, 100, 251905.	3.3	23
62	A study of the nanoscale and atomic-scale wear resistance of metallic glasses. Materials Letters, 2016, 185, 54-58.	2.6	23
63	Huge reduction of Young's modulus near a shear band in metallic glass. Journal of Alloys and Compounds, 2016, 687, 221-226.	5.5	21
64	Conductive-filler-filled poly(?-caprolactone)/poly(vinyl butyral) blends. II. Electric properties (positive) Tj ETQq0 (0 rgBT /0	verlock 10 Tf 20
65	Observation of thin film of oneâ€dimensional organic conductor tetrathiofulvalene tetracyanoquinodimethane by means of atomic force microscopy. Applied Physics Letters, 1993, 62, 1892-1894.	3.3	19
66	Nanomechanical Mapping on the Deformed Poly(ε-caprolactone). Macromolecules, 2011, 44, 1779-1782.	4.8	19
67	Probing stem cell differentiation using atomic force microscopy. Applied Surface Science, 2016, 366, 254-259.	6.1	18
68	Nanofishing of a Single Polymer Chain: Temperatureâ€Induced Coil–Globule Transition of Poly(<i>N</i> â€isopropylacrylamide) Chain in Water. Macromolecular Chemistry and Physics, 2018, 219, 1700394.	2.2	18
69	Nanoscience of single polymer chains revealed by nanofishing. Chemical Record, 2006, 6, 249-258.	5.8	17
70	Study on thermal expansion in injectionâ€molded isotactic polypropylene and thermoplastic elastomer blends. Journal of Applied Polymer Science, 2008, 107, 2930-2943.	2.6	16
71	Nanorheological Investigation of Polymeric Surfaces by Atomic Force Microscopy. Composite Interfaces, 2009, 16, 13-25.	2.3	16
72	Self-assembled porous templates allow pattern transfer to poly(dimethyl siloxane) sheets through surface wrinkling. Polymer Journal, 2012, 44, 573-578.	2.7	16

#	Article	IF	CITATIONS
73	Effect of Coexisting Covalent Cross-Links on the Properties of Rotaxane-Cross-Linked Polymers. ACS Applied Polymer Materials, 2020, 2, 1061-1064.	4.4	16
74	Direct visualization of a strain-induced dynamic stress network in a SEBS thermoplastic elastomer with in situ AFM nanomechanics. Japanese Journal of Applied Physics, 2020, 59, SN1013.	1.5	16
75	Local Mechanical Properties of Heterogeneous Nanostructures Developed in a Cured Epoxy Network: Implications for Innovative Adhesion Technology. ACS Applied Nano Materials, 2021, 4, 12188-12196.	5.0	16
76	Periodic Surface Undulation in Cholesteric Liquid Crystal Elastomers. Macromolecules, 2016, 49, 9561-9567.	4.8	15
77	Development of Flexible Cell-Loaded Ultrathin Ribbons for Minimally Invasive Delivery of Skeletal Muscle Cells. ACS Biomaterials Science and Engineering, 2017, 3, 579-589.	5.2	15
78	Nanodiamond Glass with Rubber Bond in Natural Rubber. Advanced Functional Materials, 2020, 30, 1909791.	14.9	15
79	Size-dependent elastic modulus of ultrathin polymer films in glassy and rubbery states. Polymer, 2016, 105, 64-71.	3.8	14
80	Adhesion properties of polyacrylic block copolymer pressureâ€sensitive adhesives and analysis by pulse NMR and AFM force curve. Journal of Applied Polymer Science, 2019, 136, 47791.	2.6	14
81	Conductive-filler-filled poly(?-caprolactone)/poly(vinyl butyral) blends. I. Crystallization behavior and morphology. Journal of Applied Polymer Science, 1997, 64, 797-802.	2.6	13
82	Nanorheology Mapping by Atomic Force Microscopy. Kobunshi Ronbunshu, 2005, 62, 476-487.	0.2	13
83	Young's Modulus Mapping on Hair Cross-Section by Atomic Force Microscopy. Composite Interfaces, 2009, 16, 1-12.	2.3	12
84	Silica Nanoparticle Reinforced Composites as Transparent Elastomeric Damping Materials. ACS Applied Nano Materials, 2021, 4, 4140-4152.	5.0	12
85	Structure and Properties of Biodegradable Polymer-Based Blends. Macromolecular Symposia, 2004, 216, 255-264.	0.7	10
86	Anisotropy in Thermal Expansion in Rubber Toughened Polypropylene —Injection Molded System—. Polymer Journal, 2004, 36, 563-566.	2.7	10
87	Nanorheology measurement on single circularly permuted green fluorescent protein molecule. Colloids and Surfaces B: Biointerfaces, 2005, 40, 183-187.	5.0	10
88	Nanotribology on Polymer Blend Surface by Atomic Force Microscopy. Polymer Journal, 2006, 38, 31-36.	2.7	10
89	Investigating the Dynamic Viscoelasticity of Single Polymer Chains using Atomic Force Microscopy. Journal of Polymer Science, Part B: Polymer Physics, 2019, 57, 1736-1743.	2.1	10
90	Segmented polyurethanes containing movable rotaxane units on the main chain: Synthesis, structure, and mechanical properties. Polymer, 2020, 193, 122358.	3.8	10

#	Article	IF	CITATIONS
91	Topology-transformable block copolymers based on a rotaxane structure: change in bulk properties with same composition. Nature Communications, 2021, 12, 6175.	12.8	10
92	Reinforcement Mechanism of Carbon Black-Filled Rubber Nanocomposite as Revealed by Atomic Force Microscopy Nanomechanics. Polymers, 2021, 13, 3922.	4.5	10
93	Insulating Polymer Blend Organic Thin-Film Transistors Based on Bilayer-Type Alkylated Benzothieno[3,2- <i>b</i>]naphtho[2,3- <i>b</i>]thiophene. ACS Applied Materials & Interfaces, 2022, 14, 17719-17726.	8.0	10
94	Study of the Mullins Effect in Carbon Black-Filled Styrene–Butadiene Rubber by Atomic Force Microscopy Nanomechanics. Macromolecules, 2022, 55, 6023-6030.	4.8	10
95	Biological Imaging with a Near-Field Optical Setup. Journal of Nanoscience and Nanotechnology, 2003, 3, 496-502.	0.9	9
96	Synthesis and Characterization of Aromatic Block Copolyamides by Condensative Chain Polymerization. Chemistry Letters, 2007, 36, 742-743.	1.3	9
97	Twoâ€Dimensional Skyrmion Lattice Formation in a Nematic Liquid Crystal Consisting of Highly Bent Banana Molecules. Angewandte Chemie - International Edition, 2016, 55, 11552-11556.	13.8	9
98	Mechanical property and structure of a butadiene rubber composite filled with syndiotactic polybutadiene resin. Journal of Applied Polymer Science, 2019, 136, 47934.	2.6	9
99	Model network architectures in vitro on extracellular recording systems using microcontact printing. Synthetic Metals, 2001, 117, 281-283.	3.9	8
100	A Vinylic Rotaxane Crossâ€Linker Containing Crown Ether for Hydrophilic and Hard Rotaxaneâ€Networked Polymers. Macromolecular Symposia, 2019, 385, 1800186.	0.7	8
101	Entropic and Energetic Elasticities of Natural Rubber with a Nanomatrix Structure. Langmuir, 2020, 36, 11341-11348.	3.5	8
102	Direct Observation of Poly(macromonomer) by Scanning Tunneling Microscopy*1. Japanese Journal of Applied Physics, 1996, 35, 2280-2283.	1.5	7
103	Hybrid Scanning Near-Field Optical/Tunneling Microscopy with Indium-Tin-Oxide/Au Coated Optical Fiber Probe. Japanese Journal of Applied Physics, 2002, 41, 4956-4960.	1.5	7
104	Viscoelastic maps obtained by nanorheological atomic force microscopy with two different driving systems. Japanese Journal of Applied Physics, 2018, 57, 08NB08.	1.5	7
105	Analysis of Nanomechanical Properties of Polyethylene Using Molecular Dynamics Simulation. Macromolecules, 2020, 53, 6163-6172.	4.8	7
106	Direct Visualization of Interfacial Regions between Fillers and Matrix in Rubber Composites Observed by Atomic Force Microscopy-Based Nanomechanics Assisted by Electron Tomography. Langmuir, 2022, 38, 777-785.	3.5	7
107	Single-Molecule Force Microscopy of Circularly Permuted Green Fluorescent Protein. Japanese Journal of Applied Physics, 2004, 43, 5520-5523.	1.5	6
108	Probing intra-molecular mechanics of single circularly permuted green fluorescent protein with atomic force microscopy. Ultramicroscopy, 2005, 105, 90-95.	1.9	6

#	Article	IF	CITATIONS
109	Coarse-Grained Molecular Dynamics Study of Styrene- <i>block</i> -isoprene- <i>block</i> -styrene Thermoplastic Elastomer Blends. ACS Applied Polymer Materials, 2022, 4, 2401-2413.	4.4	6
110	Evidence of the Transition from a Flexible to Rigid Percolating Network in Polymer Nanocomposites. Macromolecules, 2022, 55, 2739-2745.	4.8	6
111	Contact-induced stiffening in ultrathin amorphous polystyrene films. Polymer, 2018, 153, 521-528.	3.8	5
112	Novel Light-Illumination Scanning Tunneling Microscopy Equipped with Optical Fiber Probe. Japanese Journal of Applied Physics, 2003, 42, 4861-4865.	1.5	4
113	Coarse-grained Molecular Dynamics Simulation Study of Nanorheology and Nanotribology. Nihon Reoroji Gakkaishi, 2009, 37, 105-111.	1.0	4
114	Preparation of highâ€performance carbon nanotube/polyamide composite materials by elastic highâ€shear kneading and improvement of properties by induction heating treatment. Journal of Applied Polymer Science, 2021, 138, 50512.	2.6	4
115	Morphological characterization of the novel fine structure of the PMMA/PVDF blend. Polymer Journal, 2022, 54, 783-792.	2.7	4
116	Study of Initial Stage of Molecular Adsorption on Si(100) by Scanning Tunneling Microscopy. Japanese Journal of Applied Physics, 1996, 35, L1360-L1363.	1.5	3
117	Observation of Reconstructed Structure of Au(111) Deposited on Mica by Scanning Tunneling Microscopy. Japanese Journal of Applied Physics, 1997, 36, 326-327.	1.5	3
118	In Vitro Monitoring of Live Cardiomyocytes Dynamics by a Scanning Near Field Optical Microscope Setup. Optical Review, 1999, 6, 268-271.	2.0	3
119	Force Spectroscopy on a Single Polymer Chain. Kobunshi Ronbunshu, 2007, 64, 441-451.	0.2	3
120	Realâ€time morphological observation of isotactic polypropylene and poly(ethyleneâ€ <i>co</i> â€octene) rubber blend during temperature change. Journal of Applied Polymer Science, 2008, 108, 1857-1864.	2.6	3
121	Pulsed NMR Studies on Long-Term Crystallization Behavior and Melting Process of Natural Rubber under Elongation. Rubber Chemistry and Technology, 2008, 81, 110-120.	1.2	3
122	Viscoelasticity Analysis of Elastomer Blend Using Force Measurements of Atomic Force Microscope. Kobunshi Ronbunshu, 2012, 69, 435-442.	0.2	3
123	Sequential Selective Solvent On-Film Annealing: Fabrication of Monolayers of Ordered Anisotropic Polymer Particles. ACS Applied Materials & Interfaces, 2020, 12, 35731-35739.	8.0	3
124	INFLUENCE OF MASTICATION ON THE MICROSTRUCTURE AND PHYSICAL PROPERTIES OF RUBBER. Rubber Chemistry and Technology, 2021, 94, 533-548.	1.2	3
125	? Determination of spatial resolution of aperture-type near-field scanning optical microscope using a standard sample of quantum-dot embedded polymer film. Journal of the Korean Physical Society, 2010, 56, 1748-1753.	0.7	3
126	Polymer nanotechnology applied to polymeric nano-soft-materials. Journal of Physics: Conference Series, 2009, 184, 012030.	0.4	2

#	Article	IF	CITATIONS
127	Effect of tip radius on the nanoscale viscoelastic measurement of polymers using loss tangent method in amplitude modulation AFM. Japanese Journal of Applied Physics, 2021, 60, SE1008.	1.5	2
128	Dynamic Moduli Mapping of Rubber Blends by Nanorheological Atomic Force Microscopy. Nihon Reoroji Gakkaishi, 2020, 48, 91-99.	1.0	1
129	Correction of height-fluctuation-induced systematic errors in polymers by AFM-based nanomechanical measurements. Polymer Testing, 2021, 93, 106919.	4.8	1
130	Observation of polyaniline chains by scanning tunneling microscope in air and in liquid. , 1994, , 235-238.		1
131	Dynamic Nanofishing of Single Polymer Chains. Rubber Chemistry and Technology, 2009, 82, 271-282.	1.2	0
132	Standardization of Excitation Efficiency in Near-field Scanning Optical Microscopy. Analytical Sciences, 2011, 27, 139.	1.6	0
133	Structure and dynamics of polymeric materials in nano-scale. Chinese Journal of Polymer Science (English Edition), 2011, 29, 43-52.	3.8	0
134	Length scale of mechanical heterogeneity in a glassy polymer determined by atomic force microscopy. , 2013, , .		0
135	Metallic glass nanofibers in future hydrogel-based scaffolds. , 2014, 2014, 5276-9.		0
136	Scanning Probe Microscopy. Japanese Journal of Applied Physics, 2015, 54, 08L001.	1.5	0
137	Scanning Probe Microscopy. Japanese Journal of Applied Physics, 2017, 56, 08L001.	1.5	0
138	Atomically Controlled Surfaces, Interfaces and Nanostructures/Scanning Probe Microscopy. Japanese Journal of Applied Physics, 2019, 58, SI0001.	1.5	0
139	Cone–Paraboloid Transition of the Johnson–Kendall–Roberts-Type Hyperboloidal Contact. Langmuir, 2020, 36, 11284-11291.	3.5	0
140	Heterogeneous Viscoelasticity under Uniaxial Elongation of Isoprene Rubber Vulcanizate Investigated by Nanorheological Atomic Force Microscope and Dynamic Mechanical Analysis. Nihon Reoroji Gakkaishi, 2020, 48, 85-90.	1.0	0
141	Effect of molecular weight and architecture on nanoscale viscoelastic heterogeneity at the surface of polymer films. Polymer, 2021, 228, 123923.	3.8	0
142	Spatial Distribution of Metal Particles in Dried Metal Paste. Journal of the Japan Society of Colour Material, 2020, 93, 133-137.	0.1	0